PERGAMON

International Journal of Heat and Mass Transfer 44 (2001) 3359–3372

International Journal of HEAT and MASS TRANSFER

www.elsevier.com/locate/ijhmt

Removing the marching breakdown of the boundary-layer equations for mixed convection above a horizontal plate

Pierre-Yves Lagrée

Laboratoire de Modélisation en Mécanique, U.M.R. 7607, Université Paris VI, Boîte 162, 4 place Jussieu, Paris 75005, France

Received 8 February 1999; received in revised form 4 February 2000

Abstract

The thermal mixed convection boundary-layer flow over a flat horizontal cooled plate is revisited. It is shown that this flow is very similar to the one taking place in a free convection hypersonic boundary layer (with a shock in $x^{3/4}$): the observed singular solutions which branch out may then be reinterpreted in the framework of "triple deck" theory. Two salient structures emerge, one in double deck, if the buoyancy is very small, and the other one in single deck, if the buoyancy is O(1). These two structures are a reinterpretation of Steinrück's [J. Fluid. Mech. 278 (1994) 251–265] results. A numerical simulation of the unsteady boundary layer in the case of impulsively started and cooled plate is carried out. It leads to the separation of the boundary layer as predicted by the triple deck theory. A region of reverse flow is obtained which depends on the outflow boundary condition.

1. Introduction

Here we consider the mixed convection problem of an incompressible buoyant (following the Boussinesq approximation) fluid flowing over a semi-infinite horizontal flat plate at a constant temperature lower than the incoming flow temperature (see Fig. 1 for a definition sketch). Obviously, for a given x location, the fluid temperature, by diffusion, increases from the wall value towards that of the free stream. But for a fixed y location, the convection induces a longitudinal decrease of the temperature. The outcome is a buoyancy induced streamwise adverse pressure gradient. This gradient brakes the flow, and this creates an interaction between the thermics and the dynamics. This mechanism of mixed convection breakdown has been stated by Schneider and Wasel [30] (other examples of re-computation with different numerical methods are reviewed by Steinrück [35]); they showed that this interaction promotes a breakdown of the mixed boundary layer equation: at a relatively small abscissa, the equations are abruptly singular. Instead of a buoyant boundary layer, a buoyant wall jet may be studied; the case of adiabatic wall was studied by Daniels [10] and Daniels and Gargaro [11], and they arrived at the same conclusions. The wall jet problem is solved numerically and asymptotically by Higuera [16] who notes that the equations are not parabolic as he noted before in the case of the hydraulic jump, which is very similar in its behaviour.

To a certain extent, this self-induced braking may be explained through a retroactive process involving integral concepts as follows: as the variation of pressure is more or less proportional to the variation of the boundary layer thickness (because of buoyancy; J, defined by Eq. (1), will be the parameter), then the increase of boundary layer thickness promotes a rise in pressure, which decreases the velocity, and the result is an increase of the boundary layer thickness; the process is self-promoting. The failure of the integral method is presented in Schneider and Wasel's work [30]. Similar phenomena were observed in interacting boundary layer flows and described in [21,38] with a self-induced mechanism involving variations of boundary layer thickness and pressure (the difference being that in supersonic flows, the variations of the slope of the boundary layer give rise to pressure changes). The key mechanism in supersonic and hypersonic flows was introduced by Neiland [23] and Stewartson and Williams [40]: it is the "triple deck"

E-mail address: pyl@ccr.jussieu.fr (P.-Y. Lagrée).

0017-9310/01/$ - see front matter
PII: S0017-9310(00)00361-6

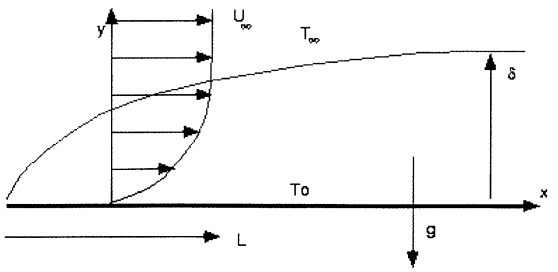

Fig. 1. Sketch of the mixed convection boundary layer flow. The temperature of the plate is different from the temperature of the flow. If the plate is cooled, the buoyancy induces an adverse pressure gradient.

theory which clarifies the scales and the equations involved in the interaction. Brown, Stewartson and Williams [7], and Brown and Stewartson [6] successfully explained the branching solutions calculated in strong hypersonic flows by Werle et al. [43] and the link with Neiland [23] (this is a free convection hypersonic boundary layer where the shock and the boundary layer behave in $x^{3/4}$). Since both the mechanism of "thermal mixed convection with low wall temperature" and of the "strongly interacting hypersonic boundary layer" seem to follow qualitatively the same path, we propose to revisit the mixed convection with the triple deck tool (see [33] for other examples).

Thermal effects in boundary layer with triple deck have been already studied in the case of stratification in the upper deck by Sykes [41] and without buoyancy by Mendez et al. [22] or on a vertical plate by El Hafi [12]. Some triple deck in mixed convection is in [18], and is extended herein.

In this paper we see (Section 3.1) that the result of the triple deck theory is that, in a mixed thermal linearized boundary layer (cold wall with very small buoyancy J), there exist eigen solutions where pressure is proportional to the displacement of the streamlines; this is like the birth of a hydraulic jump [3,13,15] or a hypersonic boundary layer [7, 13]. In the case of a hot wall, pressure is proportional to the negative of the displacement of the streamlines in the main part of the boundary layer which leads to no upstream influence but this approach captures the Tollmien Schlichting waves [32]. This triple deck result of strong self-induced upstream influence will be shown to be exactly the eigen function found by Steinrück [35] but in the limit of small J. He showed that small perturbations from the solution at a given location (before the previously computed singularity) are amplified exponentially; so the position of the singularity depends strongly on the amplification of the small numerical errors. If, thanks to a very refined calculation, the branching solutions are not selected, the buoyancy becomes greater and greater. If it is of order O(1), a self-induced interaction is again possible, but, as we will show, at different scales (Section 3.2). In this case the overall process takes place in the thin wall layer itself and there is no retroaction from the main part of the boundary layer (this is similar to what happens in pipe flows: [27,31]). This structure is similar in a certain sense to Daniels [10] and to what Steinrück [35] refers to as the "other large eigenvalues". We next examine the above breakdown using integral methods (Section 4). A solution with a back flow valid after the singular point is exhibited and discussed; links with triple deck analysis are presented.

Finally (Section 5), we present a boundary layer calculation with a simple finite difference method of the complete problem. To avoid the preceding problems unsteadiness is introduced: the plate is impulsively heated and started. We will see that a good choice in discretizing the longitudinal derivative in the equations and a good choice of outflow conditions prevent the spatial singularity: this allows the boundary layer to separate with neither evidence of finite time breakdown [42] nor instabilities. The skin friction will be shown to be coherent with Steinrück's results [35], and each of his branched solutions may be interpreted as a solution of a domain of different length.

2. Governing equations of the mixed convection

2.1. Equations

We consider an incompressible two-dimensional flow past a semi-infinite (heated or cooled) horizontal flat plate (Fig. 1). The boundary layer equations are obtained from the Navier–Stokes counter parts subject to the Boussinesq approximation for a large Reynolds number. A re-scaling of the dimensional quantities is carried out with the dynamical boundary layer scales (with $\delta = Re^{-1/2}$ with $Re = \rho_\infty U_\infty L/\mu$):

$$u^* = U_\infty u, \quad v^* = \delta U_\infty v, \quad x^* = Lx, \quad y^* = \delta L y,$$
$$p^* = p_\infty + \rho_\infty U_\infty^2 p, \quad T = T_\infty + (T_0 - T_\infty)\theta.$$

The result is the classical system (2)–(5) of thermal mixed convection [30]; Prandtl number is assumed to be of order unity and hence set (without to much loss of generality) to one while the Eckert number is assumed sufficiently small to obtain the energy equation as (5). The remaining parameter is the Richardson number or buoyancy parameter:

$$J = \frac{\alpha g (T_0 - T_\infty) L Re^{-1/2}}{U_\infty^2}, \tag{1}$$

which depends on α, the thermal coefficient of expansion of the density in the Boussinesq approximation. The transverse pressure term (4) contains the gravity term, as

Eq. (4) holds for terms greater than $O(1/Re)$, we have $|J| \gg Re^{-1}$:

$$\frac{\partial}{\partial x}u + \frac{\partial}{\partial y}v = 0, \tag{2}$$

$$u\frac{\partial}{\partial x}u + v\frac{\partial}{\partial y}u = -\frac{\partial}{\partial x}p + \frac{\partial}{\partial y}\frac{\partial}{\partial y}u, \tag{3}$$

$$0 = -\frac{\partial}{\partial y}p + J\theta, \tag{4}$$

$$u\frac{\partial}{\partial x}\theta + v\frac{\partial}{\partial y}\theta = \frac{\partial}{\partial y}\frac{\partial}{\partial y}\theta. \tag{5}$$

Boundary conditions are:

$$u(x, y=0) = 0, \quad v(x, y=0) = 0, \tag{6}$$

$$\theta(x, y=0) = \theta_w \quad \text{with} \quad \theta_w = 1, \quad u(x, y\to\infty) = 1, \quad \theta(x, y\to\infty) = 0, \; p(x, y\to\infty) = 0.$$

2.2. Marching breakdown

In this work the length scale L and the parameter J are independent, in contrast to the situation in [30] or in [11]. In the "real mixed convection problem with stable stratification flow", the "natural" longitudinal scale is effectively built with Richardson number. It is the length that gives unit Richardson number $(|\alpha g(T_0 - T_\infty) L_T U_\infty^{-2}(U_\infty L_T \nu^{-1})^{-1/2}| = 1)$, so

$$L_T = \frac{U_\infty}{\nu}\left(\frac{U_\infty^2}{-\alpha g(T_0 - T_\infty)}\right)^2.$$

Note that $J^2 L_T = L$. Schneider and Wasel [30] (scaled with L_T) showed that this system leads to a singularity when solved with a marching (in increasing x) resolution. They showed that the breakdown occurs for a rather small abscissa. This is the reason why Steinrück [35] (scaled with L_T) has investigated how the system (2)–(5) behaves when x tends to 0. In Fig. 2 are displayed, with symbols, the reduced skin friction from previous works compiled by Steinrück. The curves with numbers show solution of the marching problem with slightly perturbed initial conditions and come from his analysis near $x = 0$. Asymptotic analysis suggests, however, that it is better to consider an intermediate scale L (with $L \ll L_T$) leading to Blasius boundary layer (with this scale x tends to 0 is the nose effect) with a small thermal perturbation gauged by $|J| \ll 1$, this means that the Richardson number built with this abscissa is smaller than one. So, we will introduce the triple deck analysis.

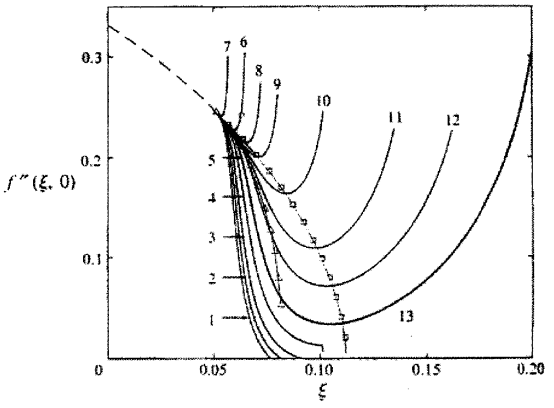

Fig. 2. The reduced skin friction compiled and computed by Steinrück (JFM 94). The numbered curves show solution of the marching problem with slightly perturbed initial conditions.

3. Asymptotic analysis: the triple deck tool

3.1. Small J, with displacement

3.1.1. Main deck

Here we look for eigen solutions in a boundary layer slightly perturbed by the thermal effect in order to show that system (2)–(5) is not parabolic in x when the plate is cooled. We use the word "parabolic" for a system of PDE in the sense of a system that can be integrated in marching in x direction from upstream to downstream (with no separation). The basic flow, driven by the free stream uniform velocity, is a classical Blasius boundary layer (thermal and dynamical effects are not coupled). We study how a localized disturbance evolves at the distance L downstream from the leading edge. At this point, the boundary layer thickness is $Re^{-1/2}L$. Pure thermal convection is relevant as long as the transverse gradient from (4) is small which implies $1 \gg |J|$. So, in this framework, the forced thermal boundary layer is of the same thickness as the dynamic one, and the velocity at station $x = 1$ is the basic Blasius velocity profile (say $U_0(y)$, the transverse variable is then the same as the self-similar one) and θ is simply $\theta_0(y) = 1 - U_0(y)$. The choice of L smaller than L_T suggests expanding in powers of a small parameter ε linked to J.

Having defined the "basic state", we follow the classical triple deck analysis [23,33,40], and more precisely [19]: system (2)–(5) is re-investigated with a smaller longitudinal scale, say $x_3 L$ (with $x_3 \ll 1$ and $x = 1 + x_3\bar{x}$); this scale is sufficiently small so that the preceding profiles may be considered as frozen. The reason for this new scale is the fact that near the breakdown point the gradient of the skin friction is infinite at scale 1, so we hope to render it O(1) at this smaller scale. This layer with height δL and length $x_3 L$ is in fact the "main deck". Next we suppose that the perturbation of longitudinal speed in the main deck is of the order of ε and the pressure of the order of ε^2, where ε is unknown (but depends on δ, J and x_3), so we recover at

these scales the inviscid problem with no longitudinal pressure gradient. The perturbations are then linked by an up to now unknown displacement function of the boundary layer called $-A(\bar{x})$ by Stewartson. In the main deck, the adimensionalized velocities and temperature up to the order of ε are:

$$u = U_0(y) + \varepsilon A(\bar{x}) U_0'(y),$$
$$v = \frac{-\varepsilon A'(\bar{x}) U_0(y)}{x_3}, \quad \theta = \theta_0(y) + \varepsilon A(\bar{x}) \theta_0'(y). \tag{7}$$

For the temperature, as for the speed, there is a matching between the outer limit of the main deck and the inner limit of the upper deck, and likewise for the bottom of the main deck and the top of the lower deck (those decks are defined later). We see that the temperature behaves as the Stewartson S function (total enthalpy) in hypersonic flows ([6,7,24]). This perturbation of temperature gives rise to a transverse change of pressure through the main deck; we develop (4) in powers of ε as follows:

$$\frac{\partial}{\partial y} p_0 + \varepsilon \frac{\partial}{\partial y} p_1 + \varepsilon^2 \frac{\partial}{\partial y} p_2 + \mathrm{O}(\varepsilon^3) = J(\theta_0(y) + \varepsilon A(\bar{x}) \theta_0(y)) + \mathrm{O}(\varepsilon^3). \tag{8}$$

At this stage, for $|J| \ll 1$ by minor degeneration (i.e. to retain the maximum of terms), we put $J = \varepsilon \tilde{J}$, because J is small with $\tilde{J}$ being a reduced Richardson number of the order of O(1). Looking at each power of ε, we see that the first term is zero (as we supposed in the Blasius Boundary layer); the second one shows that there is a pressure stratification coming from basic temperature profile ($\int_0^\infty \theta_0(y)\,\mathrm{d}y$), it does not depend on $\bar{x}$ at the short scale x_3, and it will appear that such a term can be ignored in the following analysis; the third one integrates (using $\theta_0(\infty) = 0$; $\theta_0(0) = 1$ by definition) as

$$p_2(\bar{x}, y \to \infty) - p_2(\bar{x}, y \to 0) = \tilde{J} A(\bar{x})(\theta_0(\infty) - \theta_0(0)) = -\tilde{J} A(\bar{x}),$$

where $p_2(\bar{x}, y \to \infty)$ splices with upper deck and $p_2(\bar{x}, y \to 0)$ with lower deck hitherto both being not defined. The case J of the order of one will be discussed later (Section 3.2), surprisingly, it implies again that p_1 does not drive the flow in the main deck.

3.1.2. Lower deck

From solution (7), we see that the no-slip condition is violated: $u \to U_0'(0)(y + \varepsilon A)$, and $\theta \to \theta_0'(0)(y + \varepsilon A)$ as $y \to 0$. So we introduce a new layer of thickness ε (in boundary layer scales), and scale y by $\varepsilon \bar{y}$, so the scale of u is $\varepsilon \bar{u}$ and, by least degeneracy of Eq. (2), we have $p = \varepsilon^2 \bar{p}$ (which is consistent with the matching $\varepsilon^2 p_2(\bar{x}, y \to 0) = \varepsilon^2 \bar{p}(\bar{x}, \bar{y} \to \infty)$) and v is of the order of ε / x_3. The convective diffusive equilibrium gives the relation between x_3 and ε: $x_3 = \varepsilon^3$. The problem of mixed convection near the wall is then:

$$\frac{\partial}{\partial \bar{x}} \bar{u} + \frac{\partial}{\partial \bar{y}} \bar{v} = 0, \tag{9}$$

$$\bar{u} \frac{\partial}{\partial \bar{x}} \bar{u} + \bar{v} \frac{\partial}{\partial \bar{y}} \bar{u} = -\frac{\mathrm{d}}{\mathrm{d}\bar{x}} \bar{p} + \frac{\partial}{\partial \bar{y}} \frac{\partial}{\partial \bar{y}} \bar{u}, \tag{10}$$

$$\bar{u} \frac{\partial}{\partial \bar{x}} \bar{\theta} + \bar{v} \frac{\partial}{\partial \bar{y}} \bar{\theta} = \frac{\partial}{\partial \bar{y}} \frac{\partial}{\partial \bar{y}} \bar{\theta}. \tag{11}$$

Boundary conditions are no-slip at the wall $\bar{\theta}(\bar{x}, 0) = 1$, $A(-\infty) = 0$, and for $\bar{y} \to \infty$, the matchings: $\bar{u} \to U_0'(0)(\bar{y} + A)$, $\bar{p} \to p_2(\bar{x}, y \to 0)$ and $\bar{\theta} \to 1 - U_0'(0)(\bar{y} + A)$. This set of non-linear equations is relevant in the "lower deck" of length $x_3 L = \varepsilon^3 L$ and of height $\varepsilon \delta L$ placed at station 1; here, the thermal and the dynamical problems are uncoupled. In this thin layer of small extent, the pressure coming from the main deck is the most dangerous for the velocity and may lead to separation.

3.1.3. The upper deck

3.1.3.1. Possibility of retroaction with the external flow. The perturbations of transverse velocity and pressure at the edge of the main deck introduce a perturbation in the inviscid flow: the upper deck is of size ε^3 in both directions. This perturbation is solved by the standard technique of linearized subsonic perfect fluid, this gives the Hilbert integral (the new pressure displacement relation)

$$\frac{1}{\pi} \int \frac{-A'}{\bar{x} - \xi} \mathrm{d}\xi - p_2(\bar{x}, y \to 0) = -\tilde{J} A(\bar{x})$$

and the usual gauge [33]: $\varepsilon = \delta^{-1/4} = Re^{-1/8}$ (so $J = Re^{-1/8} \tilde{J}$) and this gives the lower limit for $x_3 = Re^{-3/8}$ in Section 3.1.2. The effect of the temperature is to add a new term proportional to the displacement function A, it may be interpreted as a hydrostatic pressure variation.

3.1.3.2. Retroaction only in the boundary layer. Consideration of (7) shows that another (but equivalent) choice of ε could have been made: $\varepsilon = |J|$. With this choice, $x_3 = |J|^3$, and the preceding relation reads:

$$\frac{|J|^{-4} Re^{-1/2}}{\pi} \int \frac{-A'}{\bar{x} - \xi} \mathrm{d}\xi - p_2(\bar{x}, y \to 0) = -(|J|/J) A(\bar{x}).$$

This choice implies that we concentrate on thermal effects rather than on perfect fluid effects, if $|J| \sim Re^{-1/8}$ (note that $Re^{-1/8} \gg Re^{-1/2}$), the three terms are of the same magnitude (as seen in the preceding paragraph). Now, if $|J| \gg Re^{-1/8}$ (or $\tilde{J}$ bigger than one) there is no interaction of the boundary layer with the external

perfect fluid, the thermal effect is dominant and the pressure displacement relation degenerates in the form

$$p_2(\bar{x}, y \to 0) = \bar{p}(\bar{x}) = -A(\bar{x}) \tag{12}$$

for a cold wall ($J < 0$), and in the form

$$p_2(\bar{x}, y \to 0) = \bar{p}(\bar{x}) = A(\bar{x}) \tag{13}$$

for a hot one ($J > 0$), where in both cases $Re^{-1/8} \ll |J| \ll 1$. This shows that the upper deck is not necessary for the interaction to take place (as noted by Bowles [2]), the same phenomenon exists in free convection hypersonic flows [5,7,24] for cold wall.

3.1.4. The fundamental problem of mixed convection on "double deck" scales with displacement

Finally, the mechanism relevant for the problem of infinitely small mixed convection is without external perfect fluid retroaction, the whole process of interaction takes place in the main deck. This is a double deck interaction. We write here the final re-scaled problem (in order to avoid $U_0'(0)$). With scales

$$\begin{aligned}
x &= L + |J|^3 (L/U_0'(0))\tilde{x},\\
y &= |J|((U_0'(0))^{-2} L/Re^{1/2})\tilde{y},\\
t &= |J|^2 (L/U_\infty)\tilde{t},\\
u &= |J|((U_0'(0))^{-1} U_\infty)\tilde{u},\\
v &= (|J|^{-1}((U_0'(0))^{-2} U_\infty Re^{-1/2}))\tilde{v},\\
p &= J^2((U_0'(0))^{-2}\rho U_\infty^2)\tilde{p}
\end{aligned}$$

(and $Re^{-1/8} \ll |J| \ll 1$), the final "canonical problem of infinitely small mixed convection" is

$$\frac{\partial}{\partial \tilde{x}}\tilde{u} + \frac{\partial}{\partial \tilde{y}}\tilde{v} = 0, \tag{14}$$

$$\frac{\partial}{\partial \tilde{t}}\tilde{u} + \tilde{u}\frac{\partial}{\partial \tilde{x}}\tilde{u} + \bar{v}\frac{\partial}{\partial \tilde{y}}\tilde{u} = -\frac{\mathrm{d}}{\mathrm{d}\tilde{x}}\tilde{p} + \frac{\partial^2}{\partial \tilde{y}^2}\tilde{u}. \tag{15}$$

Boundary conditions are: no-slip at the wall ($\tilde{u} = \tilde{v} = 0$ in $\tilde{y} = 0$), no displacement far upstream ($\tilde{A} = 0$ in $\tilde{x} \to -\infty$), the matching $\tilde{y} \to \infty, \tilde{u} \to \tilde{y} + \tilde{A}$ and the coupling relation (hot wall, $\mathrm{sign}(J) = 1$, cold wall $\mathrm{sign}(J) = -1$)

$$\tilde{p} = \mathrm{sign}(J)\tilde{A}. \tag{16}$$

The introduction of time changes only the lower deck by the adjunction of the $\partial\tilde{u}/\partial\tilde{t}$ term [32]. Fig. 3 displays a rough sketch of the double deck structure.

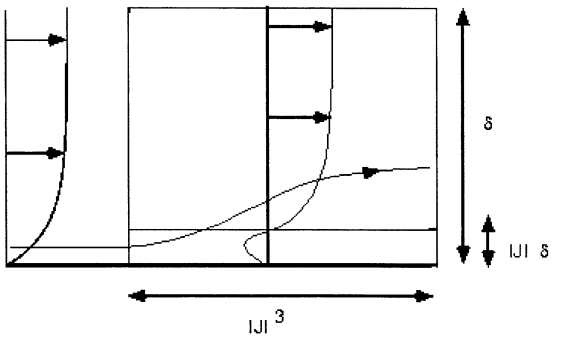

Fig. 3. The two final layers involved: the boundary layer itself and a thin wall layer.

3.1.5. Resolution

3.1.5.1. The eigenvalue solution. System (14)–(16) admits the Blasius solution $\tilde{u} = \tilde{y}$ as the basic one. Invariance by translation in space and time suggests linearized solutions of the form:

$$\tilde{u} = \tilde{y} + a\,\mathrm{e}^{\mathrm{i}(k\tilde{x} - \omega\tilde{t})} f'(\tilde{y}), \quad \tilde{v} = -\mathrm{i}ka\,\mathrm{e}^{\mathrm{i}(k\tilde{x} - \omega\tilde{t})} f(\tilde{y}),$$
$$\tilde{p} = a\,\mathrm{e}^{\mathrm{i}(k\tilde{x} - \omega\tilde{t})},$$

where $a \ll 1$. After substitution, f verifies an Airy differential equation with the variable $\eta = (\mathrm{i}k)^{1/3}\tilde{y}$, so classically we find:

$$-f'(\infty) = \frac{(\mathrm{i}k)^{1/3}}{A\,\mathrm{i}'(-\mathrm{i}^{1/3}\omega/k^{2/3})} \int_{-\mathrm{i}^{1/3}\omega/k^{2/3}}^{\infty} A\,\mathrm{i}(\zeta)\,\mathrm{d}\zeta. \tag{17}$$

3.1.5.2. Cold wall, eigenvalue and comparison with Steinrück. In the case of cold wall, the coupling ($\tilde{p} = -\tilde{A}$) gives $1 = -f'(\infty)$, and a stationary exponentially growing solution may be obtained: $\omega = 0$, $\mathrm{i}k = \Lambda = (-3A\,\mathrm{i}'(0))^3 \simeq 0.47$. We recover the same behavior as in hypersonic flows [7,13], in the birth of hydraulic jumps [3] and in supersonic pipe flows [25]. Λ is called the Lighthill eigenvalue, it shows that there is upstream influence, for example the preceding solution is the linearization of what happens far upstream of the separating point. The occurrence of eigen functions states that system (2)–(5) is not parabolic.

We have proved that the perturbation grows like $\exp[(-3A\mathrm{i}'(0))^3\tilde{x}]$. It may be compared with Steinrück's result; he showed that the system (2)–(5) scaled longitudinally by L_T admits near the origin eigen function growing like $\exp[(\lambda_0^+/\xi_0^4)\xi]$, where $\lambda_0^+ = 2U_0'(0)(-3A\,\mathrm{i}'(0))^3$, ([35, formula 2.29] or [36,A.15], with $Pr = 1$, $U_0'(0) = f''(0) = 0.33321$ and $\int_0^\infty A\,\mathrm{i}(\zeta)\mathrm{d}\zeta = 1/3$), where $\xi = (x/L_T)^{1/2}$ and where ξ_0 is the place where the flow is perturbed. If we substitute λ_0^+, ξ and ξ_0 in the exponential, bearing in mind $L/L_T = J^2$, and $|J| \ll 1$, and ξ_0 is $(L/L_T)^{1/2}$ (i.e. $|J|$), we rewrite it with our variables, and develop with the first power of $|J|$:

$$\begin{aligned}
\mathrm{e}^{(\lambda_0^+/\xi_0^4)\xi} &= \exp\left(\frac{\lambda_0^+}{|J|^3}(1 + |J|^3(1/U_0'(0))\tilde{x})^{1/2}\right)\\
&\sim \exp\left(|J|^{-3}\lambda_0^+ + \lambda_0^+(1/U_0'(0))\tilde{x}/2\right).
\end{aligned}$$

So, factorizing $\exp(|J|^{-3}\lambda_0^+)$ and substituting the value of λ_0^+, we recover the exponential growth with $\tilde{x}$:

$$\exp(-3A\mathrm{i}'(0))^3\tilde{x}.$$

So the conclusion is that the triple deck theory (which is a theory in the limit of small J at $x=1$) is equivalent to Steinrück's result (with only a different choice of scales: L_T instead of L so $J=1$ and x is small).

3.1.5.3. Non-linear resolution of the fundamental problem. The stationary and non-linear self-induced solution with $\tilde{p}=-\tilde{A}$ law is numerically computed and asymptotically described in [13]. This solution is plotted in Fig. 4, we see that the self-developing displacement $-A$ is superposed on to the pressure; the skin friction becomes negative. The upstream pressure is in $\mathrm{e}^{0.4681x}$ while the downstream is in $0.94796x^{0.4305}$ (this last behavior is noticeable very far downstream, at least $x>10^3$; these results are taken from [13]). To compute this, we use a standard Keller Box (with flare approximation) scheme for the lower deck (adapted for the triple deck from [4]). This is an inverse method which allows to catch separation: $-\tilde{A}$ is given and $\tilde{p}$ is computed. A "verse method", which is iterative (details may be found in [21], and which has been used in another hypersonic triple deck case by Lagrée [17]) is used to couple the lower deck and the pressure–deviation relation. It means that, given a displacement $-\tilde{A}^n$ at iteration level n, the next $-\tilde{A}^{n+1}$ is obtained as follows:

$$-\tilde{A}^{n+1}=-\tilde{A}^n+\lambda\left(\frac{\mathrm{d}p^n}{\mathrm{d}x}-\frac{\mathrm{d}\tilde{p}^n}{\mathrm{d}x}\right)+\mu(p^n-\tilde{p}^n),$$

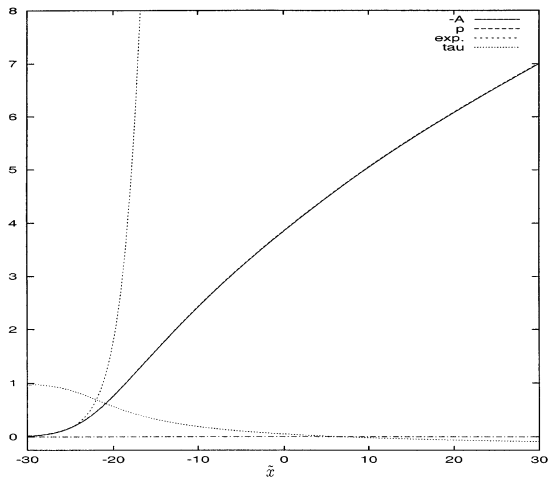

Fig. 4. Linearized eigen solution ("exp." is $\exp(-3A\mathrm{i}'(0))^3\tilde{x}$), and non-linear solution of the self induced ($\tilde{p}=-\tilde{A}$) problem solved with Keller Box and "semi-inverse" coupling: pressure (p), displacement ($-A$) and skin friction (tau).

where $\tilde{p}^n$ is the lower deck Keller Box result associated with $-\tilde{A}^n$, p^n is the pressure associated with the displacement $-\tilde{A}^n$, (here simply: $p^n=-\tilde{A}^n$, (16), with λ and μ being relaxation coefficients. These coefficients are chosen in order to stabilize the iterations: the complex gain modulus is imposed to be smaller than one for all spatial frequencies smaller than $k_{\max}=\pi/\Delta x$ (Δx is the longitudinal discretization step) and greater than π/L (L is the size of the computational domain). This gain may be written exactly in the vicinity of the null solution ($p=-A=0$ is a solution), in this case Eq. (17) gives for the Fourier transform (FT) of pressure and displacement small perturbations:

$$\mathrm{FT}(\tilde{p}^n)=(\mathrm{i}k^{1/3})\frac{FT(-A^n)}{-3A\mathrm{i}'(0)},$$

while Eq. (16) gives $\mathrm{FT}(p^n)=\mathrm{FT}(-\tilde{A}^n)$, then with $G=\mathrm{FT}(-\tilde{A}^{n+1})/\mathrm{FT}(-\tilde{A}^n)$, we have:

$$G=1+(\lambda\mathrm{i}k+\mu)\left(1-\left(\frac{(\mathrm{i}k^{1/3})}{-3A\mathrm{i}'(0)}\right)\right).$$

The choice of the coefficients λ and μ is such that, for obvious reasons of stability, $|G|<1$ for all the spatial frequencies present ($\pi/L<k<\pi/\Delta x$). The non-linear calculation is carried out with lower values for the said coefficients. Here both ends are imposed: in $x=-L/2$ and in $x=L/2$, the perturbation of $-A$ is 0 at the first step of the domain ($-L/2$), and is imposed $-A_m$ at the output ($L/2$). $L=60$ and $-A_m=7$ were largely sufficient for our purpose. The Keller Box is a marching scheme: $\mathrm{d}\tilde{p}^n/\mathrm{d}x$ is a backward derivative, the upstream influence is recovered by the derivative of the pressure $\mathrm{d}p^n/\mathrm{d}x$ which is a forward derivative.

3.1.5.4. Hot wall instability. The pressure displacement relation $\tilde{p}=\tilde{A}$ does not permit upstream influence, so the flow is now really parabolic but unstable: the dispersion equation

$$\frac{(\mathrm{i}k)^{1/3}}{A\mathrm{i}'(-\mathrm{i}^{1/3}\omega/k^{2/3})}\int_{-\mathrm{i}^{1/3}\omega/k^{2/3}}^{\infty}A\mathrm{i}(\zeta)\,\mathrm{d}\zeta=1$$

gives $\omega=2.3$ and $k=1.0$. The scaled values for a neutral Tollmien–Schlichting wave are then $\omega^*=2.3|J|^{-2}(U_0^*/L)$, and $\lambda^*=18.9|J|^3L$.

3.2. Bigger J with no displacement

3.2.1. New main deck

The preceding structure is characterized by the interaction between the lower deck and the main deck by a pressure–displacement function: the pressure in the lower deck produces a displacement which changes the pressure again in the main deck, and so on. Here in discussing relation (8), we confine the interaction in the

lower deck itself, without retroaction in the main deck. This idea is in fact deduced from Steinrück and from Daniels [10]. The latter author has found the self-similar solution U_0, p_0 and θ_0 associated to a problem with a superposition of a jet and a constant flow with an adiabatic wall. Numerical explosions with a marching scheme were observed which lead him to investigate the corresponding eigenvalue problem for the said flow.

Up to now, pressure was found to be of the order of ε^2, while perturbations of u velocity component and displacement $-A$ in the main deck were found of order ε. Similar interaction appears in pipe flows in the presence of a bump, without thermal effect, (see [27,31]). The bump gives rise to perturbation of pressure (of order ε^2) with no displacement in the main deck (at order ε): $-A = 0$. This $O(\varepsilon^2)$ pressure drives perturbations in the main deck of $O(\varepsilon^2)$ in velocity, and so a $O(\varepsilon^2)$ displacement.

If now we introduce thermal effects and if J is small, the conclusion is the same: $-A = 0$ in the main deck at order ε. Now if J becomes of order unity ($J = O(\varepsilon^0)$), relation (8) suggests that the perturbation of pressure is of order ε. But, because of the $O(\varepsilon)$ matching of velocities between lower and main deck, the pressure in the lower deck is always of order ε^2. Thus the matching of pressure implies again that there is no εp_1 contribution: there is again no displacement εA at first order (it is the same as in the "double deck" structure pointed out before). With no anticipation, we put here ε^α for the order of the perturbations in this new deck, with $\alpha > 1$ (the complete analysis will show that the matching with the lower deck will give surprisingly $\alpha = 3/2$ and not 2 as in pipe flows); here U_0, p_0 and θ_0 denote the solution (as computed by Daniels) with x scaled by L_T, and y by δL_T (boundary layer thickness in L_T scales, Re is computed with L_T) that is perturbed. As the scale is L_T, in this section J stands for sign(J).

$$u = U_0(y) + \varepsilon^\alpha u_\alpha, \quad v = \frac{\delta\varepsilon^\alpha}{x_3} v_\alpha, \quad p = p_0 + \varepsilon^\alpha p_\alpha,$$
$$\theta = \theta_0 + \varepsilon^\alpha \theta_\alpha, \quad x = 1 + x_3\hat{x}, \quad y = y.$$

As long as $1 \gg \varepsilon \gg Re^{-1/6}$, the main deck problem is different because the longitudinal gradient of pressure is still present:

$$\frac{\partial}{\partial\hat{x}} u_\alpha + \frac{\partial}{\partial y} v_\alpha = 0, \tag{18}$$

$$U_0(y)\frac{\partial}{\partial\hat{x}} u_\alpha + v_\alpha U_0'(y) = -\frac{\partial}{\partial\hat{x}} p_\alpha, \tag{19}$$

$$0 = -\frac{\partial}{\partial y} p_\alpha + J\theta_\alpha, \tag{20}$$

$$U_0(y)\frac{\partial}{\partial\hat{x}} \theta_\alpha + v_\alpha \theta_0'(y) = 0, \tag{21}$$

where $U_0(y)$ solves the mixed convection problem. If we define ψ_α the perturbation of the stream function, θ_α is straightforward: $\theta_\alpha = \psi_\alpha(\hat{x}, y)\theta_0'(y)/U_0(y)$. After elimination of the velocities and pressure, we have to solve a modified Rayleigh equation:

$$\frac{\partial^2}{\partial y^2}\psi_\alpha - \left(\frac{U_0''(y)}{U_0(y)} - J\frac{\theta_0'(y)}{U_0^2(y)}\right)\psi_\alpha = 0. \tag{22}$$

This equation may be solved in y in assuming zero perturbation at the outer edge (for sake of simplicity we suppose that there is no upper deck of perturbed perfect fluid involving the Hilbert integral) and the matching for p_α in $y = 0$ is discussed later. The value of $u_\alpha(\hat{x}, 0)$ will not interfere with the lower deck.

If $\delta\varepsilon^2/x_3^2 = \varepsilon^2/\delta$, then the transverse velocity v_α is present too in the transverse pressure gradient equation (20), so it is now

$$U_0(y)\frac{\partial}{\partial\hat{x}} v_\alpha = -\frac{\partial}{\partial y} p_\alpha + J\theta_\alpha;$$

the equation for ψ_α may be then obtained. If this term is in the equations, then we have $x_3 = \delta = Re^{-1/2}$ and $\varepsilon = Re^{-1/6}$, and the main deck has same scales in both directions.

3.2.2. New lower deck: the fundamental problem of mixed convection on "single deck" scales with no displacement

For the sake of simplicity we put $U_0'(0) = 1$ and $|\theta_0'(0)| = 1$. The lower deck problem is then changed by the fact that the transverse pressure variation is within the lower deck, (in Section 3.2.1, the transverse variation of pressure took place in the main deck), it is a single deck interaction:

$$u = \varepsilon\hat{u}, \quad v = \varepsilon^2\hat{v}, \quad p = p_\infty + J\varepsilon\hat{y} + \varepsilon^2\hat{p}_2,$$
$$\theta = 1 + \varepsilon\hat{\theta}, \quad x = 1 + \varepsilon^3\hat{x}, \quad y = \varepsilon\hat{y},$$

(because $x_3 = \varepsilon^3$),

$$\frac{\partial}{\partial\hat{x}}\hat{u} + \frac{\partial}{\partial\hat{y}}\hat{v} = 0, \tag{23}$$

$$\hat{u}\frac{\partial}{\partial\hat{x}}\hat{u} + \hat{v}\frac{\partial}{\partial\hat{y}}\hat{u} = -\frac{\partial}{\partial\hat{x}}\hat{p}_2 + \frac{\partial^2}{\partial\hat{y}^2}\hat{u}, \tag{24}$$

$$0 = -\frac{\partial}{\partial\hat{y}}\hat{p}_2 + J\hat{\theta}, \tag{25}$$

$$\hat{u}\frac{\partial}{\partial\hat{x}}\hat{\theta} + \hat{v}\frac{\partial}{\partial\hat{y}}\hat{\theta} = \frac{\partial^2}{\partial\hat{y}^2}\hat{\theta}. \tag{26}$$

The matching is $\hat{u} \to \hat{y}$ and $\hat{\theta} \to -\hat{y}$, for $\hat{y} \to \infty$, because there is no displacement. At the wall, the boundary conditions are obvious: $\hat{u} = \hat{v} = \hat{\theta} = 0$. The pressure matches at order ε^2, that is the value of the lower deck

pressure for $\hat{y} \to \infty$ which makes the main deck develop, and there is no retroaction from the main deck to the lower one. All the problem lies in the lower deck: there is no need for an external pressure change (because here $\partial \hat{p}_2/\partial \hat{y} \neq 0$). This is true for any ε in the range $1 \gg \varepsilon \geqslant Re^{-1/6}$.

3.2.3. Linearized resolution

Branching solutions are obtained from the linearized system deduced from (23)–(26), where (u, v, p_2, θ) denotes perturbations from the basic state $(\hat{y}, 0, 0, 0, 0)$ (here J is sign(J)):

$$\frac{\partial}{\partial \hat{x}} u + \frac{\partial}{\partial \hat{y}} v = 0, \tag{27}$$

$$\hat{y} \frac{\partial}{\partial \hat{x}} u + v = -\frac{\partial}{\partial \hat{x}} p_2 + \frac{\partial^2}{\partial \hat{y}^2} u, \tag{28}$$

$$0 = -\frac{\partial}{\partial y} p_2 + J(\theta), \tag{29}$$

$$\hat{y} \frac{\partial}{\partial \hat{x}} \theta + v = \frac{\partial^2}{\partial \hat{y}^2} \theta. \tag{30}$$

This suggests looking for solutions in the form:

$$u = \mathrm{e}^{\kappa x} \phi'(\hat{y}), \quad v = -\kappa \mathrm{e}^{\kappa x} \phi(\hat{y}), \quad p_2 = J(g(\hat{y}))\, \mathrm{e}^{\kappa x},$$
$$\theta = \mathrm{e}^{\kappa x} g'(\hat{y}),$$

with the pressure value given at the wall (as the system is linear we simply write $g(0) = 1$). κ is the eigenvalue that we are looking for. We note that the system may be written as:

$$\left(\frac{\partial}{\partial \hat{y}} \frac{\partial}{\partial \hat{y}} - \kappa \hat{y} \right) g'(\hat{y}) = \kappa \phi(\hat{y}),$$
$$\left(\frac{\partial}{\partial \hat{y}} \frac{\partial}{\partial \hat{y}} - \kappa \hat{y} \right) \phi''(\hat{y}) = J \kappa g'(\hat{y}). \tag{31}$$

If we write $\eta = \kappa^{1/3} \hat{y}$, so that κ disappears from the problem, any κ is convenient. The problem is solved numerically for $J = -1$ by a finite difference method with time reintroduced to provide for a relaxation mean of the numerical scheme. In Fig. 5, the computed velocity profile $\phi'(\eta)$ is compared with the corresponding asymptotic solution while temperature results, $g'(\eta)$, are shown in Fig. 6, (no solution was found with this method for $J = 1$). The profiles of velocity and temperature slowly decrease in oscillating to 0 as $\eta \to \infty$. This is coherent with the leading term of ϕ which is in η^n, where n solves $n^2 - n + 1 = 0$. Hence ϕ involves $\eta^{(1 \pm \mathrm{i}\sqrt{3})/2}$ as $\eta \to \infty$, thereby implying that v is proportional to $\sqrt{\eta} \sin(\sqrt{3} \log(\eta)/2)$, and by consequence u becomes proportional to $-(\mathrm{d}/\mathrm{d}\eta)(\sqrt{\eta} \sin(\sqrt{3} \log(\eta)/2))$ and θ to $(-1/\sqrt{\eta}) \sin(\sqrt{3} \log(\eta)/2)$ (the exact coefficient of proportionality has not been determined).

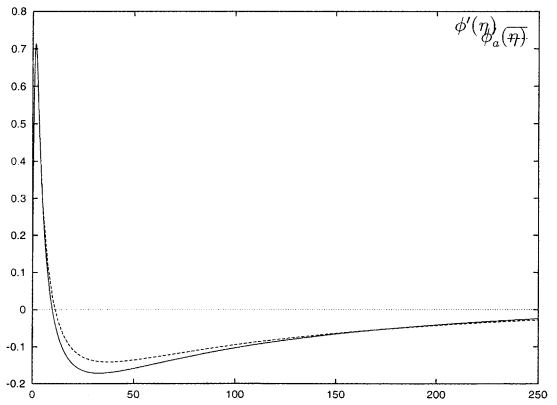

Fig. 5. Comparison of the computed value of $\phi'(\eta)$ and asymptotic value

$$\phi'_{\mathrm{a}}(\eta) = \frac{-(\sqrt{3} \cos(\frac{\sqrt{3} \log(\eta)}{2})}{2\sqrt{\eta}} - \frac{\sin(\frac{\sqrt{3} \log(\eta)}{2})}{2\sqrt{\eta}}.$$

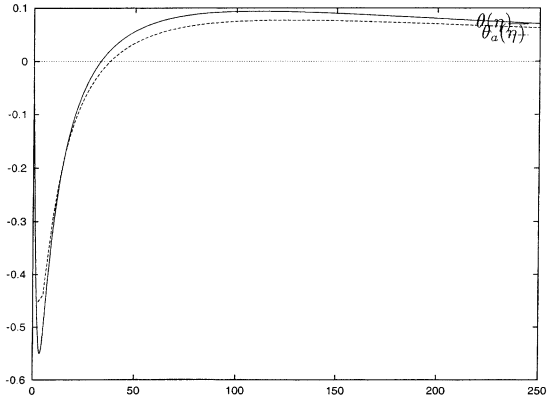

Fig. 6. Comparison of the computed value of $\theta(\eta)$ and asymptotic value

$$\theta_{\mathrm{a}}(\eta) = \frac{-(\sin(\frac{\sqrt{3}\ \log(\eta)}{2})}{\sqrt{\eta}}.$$

Let us return now to the matching of the two layers in order to obtain α. In the lower deck the pressure is $\mathrm{O}(\varepsilon^2)$, and behaves for large $\hat{y}$ like $\sqrt{\hat{y}}$, so, written in outer variables the pressure becomes $\varepsilon^2 \sqrt{\hat{y}} \sim \varepsilon^{3/2} \sqrt{y}$. In the vicinity of $y = 0$, (22) behaves as

$$\frac{\partial^2}{\partial y^2} \psi_\alpha + J \frac{1}{y^2} \psi_\alpha \simeq 0.$$

If $J = -1$, ψ_α involves the same powers of y as η: $y^{(1 \pm \mathrm{i}\sqrt{3})/2}$, and hence θ_α is proportional to combinations of $y^{(-1 \pm \mathrm{i}\sqrt{3})/2}$ and the pressure (of order ε^α) contains the square root of y. Matching of the pressure between the two decks leads to $\alpha = 3/2$. With perturbation of order $\varepsilon^{3/2}$ the other matchings are straightforward. We

conclude that any value of κ is acceptable and creates a self-induced solution in the lower deck with no first-order displacement: the dominant variations of velocities and pressure are confined in the lower deck, the main deck is passive.

3.2.4. Comparison with Daniels and Steinrück results

Daniels solves a set of equations closely related to the preceding one, and without reference to triple deck. The main difference is that he chooses non-linear profiles: $U_0(y) \simeq y^{b-1}$ and $\theta_0(y) \simeq \theta_0(0) + y^c$, near $y = 0$. This may be interpreted as a thicker lower deck (the matching is not in the linear region but somewhere higher). So the longitudinal scale is now $x_3 = \varepsilon^{b+1}$. The adiabaticity gives in his study $(-(\partial/\partial\hat{y})p_2 = 0)$. He finds which exact power b of $\hat{y}$ is coherent for the lack of what we would call the displacement function and that he calls "an origin shift" in the transversal variable and noted as $k_3(b)$. Thus he shows that $k_3(b) = 0$ is necessary for the matching of the two layers. As a result, near the singularity, in $\hat{x} < 0$, the eigen function of the pressure is found to be $\simeq (-\hat{x})^{0.305}$ and there is a free interaction with decreasing pressure.

Nevertheless, here we deal with $b = 1$; instead of 0.305 we find 1/3. We note that if $b = 1$ in Daniels's results, there is no perturbation at all (see Fig. 4 in [10, p. 431], where, when the pressure noted as q equals zero, the displacement, noted as $k_3(b)$, equals zero as well); this is the same here, if there is no transverse variation of pressure, there is no possible linearized solution in the lower deck with $-A = 0$ except the null solution.

This solution is in fact what Steinrück calls the other large eigenvalues, the oscillating behavior [35, Eq. (3.12)] involves $1/2 \pm \mathrm{i}\sqrt{3/4}$ (it is the same because we took $|\theta_0'(0)|/U_0'(0)^2 = 1$). So, the two sets of eigenvalues are explained by a triple deck analysis.

4. Integral methods and branching solutions

4.1. Singularity

The preceding results for small J suggest that there is no singularity in the equations, but because of non-parabolicity, a dependence with downstream conditions. The flow may generate a self-induced interaction which may lead to separation (at least in the $\tilde{p} = -\tilde{A}$ case). So, we may revisit the over-simplification of the problem with integral methods as already mentioned by Schneider and Wasel [30], to see whether we may go after the singularity even in this very simple description. They integrate over the whole boundary layer the system (2)–(5) as follows:

$$\frac{\mathrm{d}}{\mathrm{d}x}\int_0^\infty \left[u(1-u) + J\int_y^\infty \theta\,\mathrm{d}Y\right]\mathrm{d}y = \left(\frac{\partial u}{\partial y}\right)_{y=0}.$$

This balance may be rewritten with the help of the displacement function δ_1 (which is more physical in our opinion):

$$\frac{\mathrm{d}}{\mathrm{d}x}\left[\frac{\delta_1}{H} + JA\delta_1^2\right] = \frac{f_2 H}{\delta_1}, \tag{32}$$

where H and f_2 are standard notations [28]; $H = \delta_1/\delta_2$ is by definition the shape factor, and f_2 is defined from the skin friction as $f_2 = \delta_2(\partial u/\partial y)_{y=0}$. Now the problem must be solved with assumptions on the profile shape. Classically f_2 is a function of H and H is the function of the pressure gradient and δ_1. Like Schneider and Wasel, we choose a simple sinusoidal profile with constant parameters ($H = H_0$, $A = A_0$ and $f_2 = f_{20}$). The profile $u = \sin(\pi(y/\delta))$ permits to evaluate $H_0 = 2(2-\pi)/(\pi-4)$ and $f_{20} = 1 - \pi/4$, the value of A_0 is $(-8+\pi^2)/(2(-2+\pi)^2)$.

Then the integral equation (32) integrates in:

$$\left(\frac{1}{2}(\delta_1^2 - \delta_{10}^2) + \left(\frac{2}{3}\right)JH_0A_0(\delta_1^3 - \delta_{10}^3)\right) = f_{20}H_0^2(x - x_0).$$

At the leading edge $x_0 = 0$ and $\delta_{10} = 0$, so we may obtain an explicit δ_1 as a function x. It is much more simple to plot $(x(\delta_1), \delta_1)$ in a parametric mode. The case $J = 0$ reduces of course to the approximation of the Blasius solution:

$$\delta_{1B} = \sqrt{2f_2H_0^2}x^{1/2} = 1.742x^{1/2}$$

and for a non-zero negative J we find, with Schneider and Wasel, that there is a singularity in the slope $(\mathrm{d}\delta_1/\mathrm{d}x) = \infty$ in $x_s = (24A_0^2H_0^4f_2J^2)^{-1}$, where $\delta_1 = -1/(2A_0H_0J) = \delta_s$ say, which is finite).

4.2. Non-singular solution

Schneider and Wasel stopped with x_s, but we may construct the sequel of the solution after x_s if we note that for $x > x_s$ the solution may be integrated if $f_2 < 0$ (say $f_2 = f_{2s}$). For the sake of oversimplification, we only change the value of f_2 in (32), the solution reads:

$$\left(\frac{1}{2}(\delta_1^2 - \delta_s^2) + \left(\frac{2}{3}\right)JH_0A_0(\delta_1^3 - \delta_s^3)\right) = f_{2s}H_0^2(x - x_s).$$

This expression is singular in x_s and valid for $x > x_s$. In Fig. 7, we plot the two expressions of δ_1 (upstream and downstream of x_s) and δ_{1B} on the same graph.

Thus we have a continuously varying δ_1 valid throughout except in x_s. The displacement shows a gradual increase as long as the thermal effect is small, then it thickens in the vicinity of the separation, and finally it slowly increases. We note that it looks like a "jump" in the displacement thickness.

4.3. Branching solutions

Of course, a better description should involve a continuously varying H and f_2 (this will enable to cross x_s). As a first step in this direction, we present an over-simplified argument – we may develop the shape factor (only in the right-hand side, in the left-hand side it has no real influence) near the Blasius value as follows: $H = H_0 - Jh(\mathrm{d}\delta_1/\mathrm{d}x)$. We may justify this postulate in noticing that for a small adverse pressure gradient a small growth of H is promoted (this is true in a classical boundary layer such as the Falkner Skan's one where $H_0 \simeq 2.59$ and $h \simeq 2.88\ldots$), but here the variation of pressure through the boundary layer is more or less proportional to $J\delta_1$; this introduces a parameter $h > 0$. With these crude assumptions and at first order in J, a new term appears, proportional to the second derivative of the displacement:

$$\frac{\mathrm{d}}{\mathrm{d}x}\left[\frac{\delta_1}{H}\right] \simeq Jh\left[\frac{\delta_1}{H_0^2}\right]\frac{\mathrm{d}^2\delta_1}{\mathrm{d}x^2} + \frac{\mathrm{d}}{\mathrm{d}x}\left[\frac{\delta_1}{H_0}\right];$$

so (32) is now

$$Jh\left[\frac{\delta_1}{H_0^2}\right]\frac{\mathrm{d}^2\delta_1}{\mathrm{d}x^2} + \left[\frac{1}{H_0} + 2JA\delta_1\right]\frac{\mathrm{d}}{\mathrm{d}x}\delta_1 \simeq \frac{f_2H_0}{\delta_1}.$$

With this ad hoc term in the equation, first, the singularity will be smoothed (for example, we may construct an asymptotic description of the equation in introducing a region in x_s where $(\mathrm{d}^2\delta_1/\mathrm{d}x^2)$ is not negligible…), and second, closely linked eigen function may be exhibited if we write $\delta_1 = \delta_{10}(1 - a\mathrm{e}^{Kx})$, where δ_{10} is the Blasius solution frozen (K must be big) and K solves

$$hJ\left[\frac{\delta_{10}}{H_0^2}\right]K^2 + K\left(\frac{1}{H_0} + 2JA\delta_{10}\right) + \frac{f_2H_0}{\delta_{10}} \simeq 0.$$

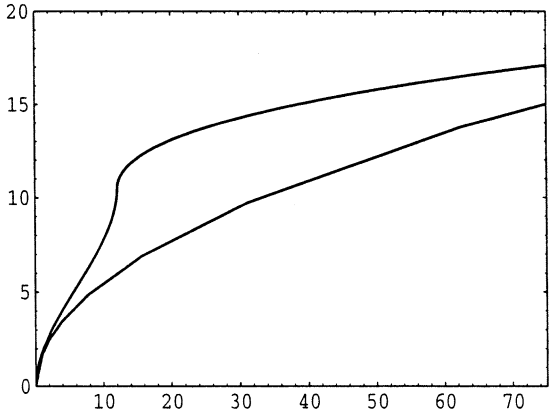

Fig. 7. The upper curve is the plot of δ_1 function of x as predicted by the very simple model, the lower one is the Blasius solution.

The roots, for small J are at first order $-(f_2H_0^2)/\delta_{10}$ and $(-J)^{-1}(H_0/h\delta_{10})$. If J is positive, they are negative, so any perturbation is damped, and the parabolic nature of the flow is recovered. If J is negative, the first one remains negative, but the other is positive and big leading to a growing exponential on a short scale. This solution destroys the parabolicity of the flow, and is clearly a consequence of the h term. This behavior, qualitatively similar to the complete resolution (as we will see in the next paragraph) and with the occurrence of branching exponential solutions (as in triple deck), shows again how powerful the integral methods are [21] if the variation of H with the pressure gradient is not omitted. In the next section, we look at how the previous results may be observed on a complete numerical simulation of the equations, and whether it is possible to obtain a separated flow.

5. Numerical computations

5.1. The problem

As shown in the previous paragraph with different scales and methods, solving the equations with a marching scheme in x (stationary in t) leads to the selection of the eigenvalues and to a self-induced interaction. In supersonic flows, the way to prevent this fact is to construct an iterative coupled method as already mentioned. It permits to impose boundary conditions at both ends of the domain. Here the problem is that the pressure changes across the boundary layer, so these powerful methods are not applicable. We propose to change the problem and to make it unsteady.

We have to solve (2)–(5) with the ∂_t term and new boundary conditions at $t = 0$ and at $x \to \infty$:

$$\frac{\partial}{\partial x}u + \frac{\partial}{\partial y}v = 0, \tag{33}$$

$$\frac{\partial}{\partial t}u + u\frac{\partial}{\partial x}u + v\frac{\partial}{\partial y}u = -\frac{\partial}{\partial x}p + \frac{\partial}{\partial y}\frac{\partial}{\partial y}u, \tag{34}$$

$$0 = -\frac{\partial}{\partial y}p + J\theta, \tag{35}$$

$$\frac{\partial}{\partial t}\theta + u\frac{\partial}{\partial x}\theta + v\frac{\partial}{\partial y}\theta = \frac{\partial}{\partial y}\frac{\partial}{\partial y}\theta, \tag{36}$$

with, at time $t = 0$:

$$u(x, y > 0, t = 0) = 1, \quad u(x, y = 0, t = 0) = 0,$$

$$v(x, y \geqslant 0, t = 0) = 0, \quad \theta(x, y > 0, t = 0) = 0,$$

$$p(x, y \geqslant 0, t = 0) = 0,$$

and after, for $t > 0$:

$$u(x, y = 0, t \geqslant 0) = 0 \quad v(x, y = 0, t \geqslant 0) = 0,$$
$$u(x, y \to \infty, t \geqslant 0) = 1, \quad \theta(x, y = 0, t \geqslant 0) = 1,$$
$$\theta(x, y \to \infty, t \geqslant 0) = 0, \quad p(x, y \to \infty, t \geqslant 0) = 0,$$

$$\forall y, \text{ for } x > t, x \to \infty : \frac{\partial}{\partial x} u = 0, \quad \frac{\partial}{\partial x} v = 0, \quad \frac{\partial}{\partial x} p = 0,$$
$$\frac{\partial}{\partial x} \theta = 0.$$

If, at a given x, we wait for a long time, and with a big enough domain, we expect to find a steady solution which solves (2)–(5) too after a transient spreading.

5.2. Numerical discretization

The set of (33)–(36) is discretized in finite differences in the most simple way, second order in space x, y and in time t. It is implicit in y and explicit in x. We introduce an internal loop to improve the description of the non-linear terms put as explicit source terms.

The first difficulty is now at the entry: we cannot begin the calculation in $x = 0$ because the equations are singular at the origin, so we impose the Blasius boundary layer profile at any time $t > 0$, in $x = x_{\text{in}} > 0$. This creates a small non-dangerous perturbation.

The second one is at the exit, where $x = x_{\text{out}}$. The annulation of longitudinal derivatives ($\partial/\partial x = 0$) at the outlet is a coherent boundary condition as long as no information has propagated (at velocity 1) from the nose. If $t > x_{\text{out}}$, it is not true anymore.

The third difficulty is the numerical discretization in x. If we put a centered derivative $((f^N_{i+1j} - f^N_{i-1j})/2\Delta x)$ we observe oscillations; by inspection, if we choose a downstream derivative $((3f^N_{ij} - 4f^N_{i-1j} + f^N_{i-2j})/2\Delta x)$ in the transport equations but we center $v^{N+1}_{ij} = -((\psi^{N+1}_{i+1j} - \psi^{N+1}_{i-1j})/2\Delta x)$ in the incompressibility, no oscillations are observed and the back flow region is computed.

6. Results

6.1. Test cases

As a test case of our numerical discretization (for the unsteady part as well for the non-linear part), we have recomputed the classical problem of the starting flat plate (solved analytically by Stewartson [37,39] and numerically by Hall [14]).

For the sake of validation of boundary layer separation phenomena, we have computed the starting flow around a cylinder. We recover the Van Dommeln and Shen [42] result of finite time singularity. For this severe test, the three different discretizations in x were tested. We conclude that the effect of the choice of the longitudinal derivative (centered or not) on the position of the separating point is very small: a difference of 0.3%. In [20] we discuss more precisely those examples. Of course, this finite difference scheme in Eulerian description does not go near the singularity as Cassel et al. [8] do with boundary layer equations written in Lagrangian description. Nevertheless, it predicts the singularity, so this is an element of validation of the back flow calculation.

Next, we introduce the transverse buoyancy, but we impose the temperature to be $x^{-1/2}$ rather than 1. For example if $J = -0.025$ we obtain $\delta_1 \simeq 1.9x^{1/2}$ and $\partial u/\partial y(x, 0) \simeq 0.29x^{-1/2}$; the value $\partial u/\partial y(x, 0)\sqrt{x}$ as a function of $|J|\sqrt{x}$ for different time steps is plotted in Fig. 8 (the choice of abscissa $\xi = |J|\sqrt{x}$ and ordinate $f''(\xi, 0) = \partial u/\partial y(x, 0)\sqrt{x}$ comes from Steinrück's work based on self-similar variables).

The lines correspond to the Rayleigh solution of the problem: an infinite flat plate impulsively moved and heated. In this case $(\sqrt{x}(\partial u/\partial y)(x, y = 0) = -1\sqrt{\pi x/t}$, which is linear in $|J|\sqrt{x}$ and whose slope decreases with time t), they are plotted for comparison (so we see the propagation of the influence of the nose). We note that it takes a long time to obtain the stationary (here self-similar) solution computed by Schneider [29] and Afzal and Hussain [1], this flow is a particular case of the generalized Falkner Skan mixed convection as pointed out by Ridha [26]. The last points present a small discrepancy because of the output effect: the upstream influence of $(\partial/\partial x)p = 0$.

This is an element for the validation of the thermal coupling part of our dicretization. Note, that for

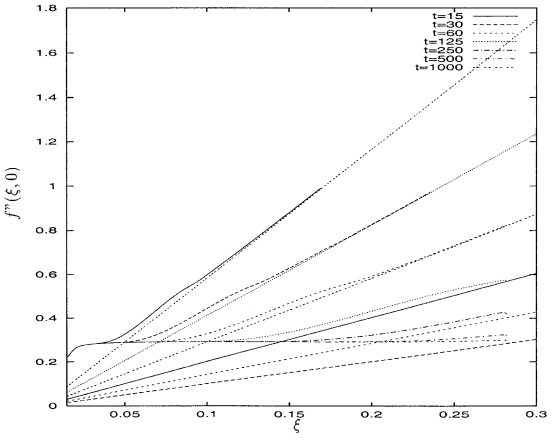

Fig. 8. Numerical computation of the reduced skin friction function as a function of the reduced longitudinal variable at different times (from $t = 15$ to 3000) and in the case of wall temperature $T_w(x) = 1/\sqrt{x}$. The reduced Rayleigh skin friction is plotted as well (lines at time $t = 15, 30, 60, 125, 250, 500$ and 1000. The final value is the self-similar one: 0.29).

$-0.8 \simeq< J < 0$ there are two self-similar solutions, one with a positive skin friction and an other with a negative skin friction [26,36]. Steinrück [36] showed that it is possible, near the critical value, to branch from the self-similar flow (for $x \to 0$) with positive skin friction to the other, with negative skin friction (at large x).

6.2. Starting flow, buoyant, non-self-similar results

In the sequel, we fix $J = -0.025$. The temperature of the wall is equal to 1. This value of J is a compromise between two effects: first, if J is too large, the interaction takes place near the nose where the gradients are big, Δx must be not too small and x_{in} must also be not too small; second, if J is too small, the Blasius part is well solved, but the size of the computational domain is now too big. $J = -0.025$ seems to be good enough to prevent those two drawbacks.

In Fig. 9, we display the converged reduced skin friction at the wall as function of the size of the domain (i.e. the value of x_{out}). We note that, depending on this size, we obtain different solutions. The first points present an error coming from the discretization at the input, they are not far from $f''_{\text{Blasius}}(0) = 0.33$. Reducing the step size decreases this error (the error is amplified on the graph because of the $\sqrt{x}$ term coming from $\xi = |J|\sqrt{x}$). The quantity $f''(\xi, 0) = (\partial u/\partial y)(x, 0)\sqrt{x}$ decreases to a minimum and increases greatly after and reaches a maximum at the end of the computational zone. This minimum decreases as the size of the domain increases and ultimately this leads to separation. Finally, we may compare favorably results from Fig. 9 and Steinrück's results [35, p. 261, Fig. 1] reproduced in Fig. 2: most of the curves have common parts with Wickern results compiled by Steinrück. But here the originality of our work is that we catch the back flow, so our curves do not stop at separation.

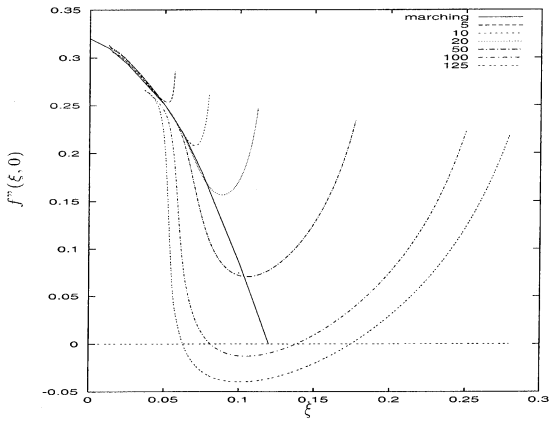

Fig. 9. The reduced skin friction function of the domain size. Results are compared with the calculation of Wickern (1991) (compiled by Steinrück) and referred as marching. The size of the domain is $x_{\text{out}} = 5$ 10, 20, 50, 100 and 125.

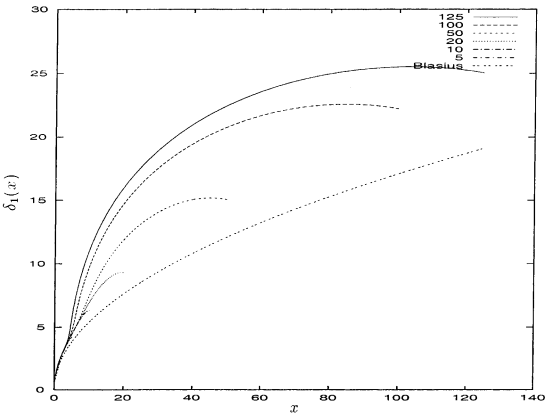

Fig. 10. The displacement thickness $\delta_1(x)$ for several domain sizes ($x_{\text{out}} = 5$ 10, 20, 50, 100 and 125).

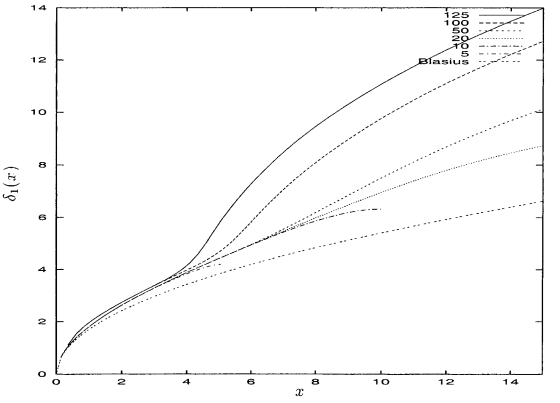

Fig. 11. The displacement thickness $\delta_1(x)$ for several domain size, from the nose to $x = 15$.

In Fig. 10, we plot the displacement thickness as a function of x (final state) for the different domain sizes compared with Blasius solution. Fig. 11 is a zoom of the same figure showing the sudden increase of displacement thickness associated to the boundary layer separation.

We do not observe any singularity at a finite time as observed in all the boundary layer calculation for impulsive flow [42]. In investigating smaller grid effects, we do not observe oscillations as predicted by Cowley et al. [9] or Smith and Elliot [34].

7. Conclusion

This problem is very interesting because it summarizes all the difficulties of boundary layer flows: the existence of eigen function destroying the parabolicity,

boundary conditions difficult to settle, occurrence of a back flow, and numerical and physical instabilities.

Numerical calculations with marching techniques have clearly shown [35] that there is a singularity in the self-interaction of the boundary layer for $J = O(1)$. This singularity is similar to the "branching solutions" obtained in supersonic inviscid–viscous interacting flows (and presented by Werle et al. [43]). These interacting boundary layer flows were often solved with integral methods, and we have presented here such a simplified resolution too. The divergence of the numerical solution was observed, and often explained with those integral methods [21]. As we have exactly the same behavior as clearly stated by Steinrück who compares a lot of numerical results, we have presented here the same arguments: we have showed that integral methods may be extended to remove the singularity (as in aerodynamics), we have showed that this behavior is natural from the triple deck theory (in aerodynamics, the supersonic and hypersonic boundary layer flows were the problems which have led Neiland and Stewartson to introduce the triple deck analysis).

Two different asymptotic structures were presented, the first with small J predicts that there is no singularity but amplification of any perturbation; the second at J of the order of one predicts a self-similar singularity at any location. These two structures were shown to be those found by Steinrück but with a different approach. Moreover, we have presented a numerical computation showing that the self-induced singularity may be removed if downstream conditions are supplied (coherent with the first mechanism: amplification of any perturbation at small J). No general physical boundary conditions were imposed, nevertheless with a zero gradient output condition, we showed that depending upon the size of the domain a different branching solution may be selected. The boundary layer may then separate and present a region of back flow (even after step size reduction, no oscillations were observed). This is a generalization of Steinrück results.

Some questions may arise, first of physical interpretation: does this upstream influence describe the phenomenon of "blocking" which is observed in stratified flows? Is it the result of the existence of a kind of hydraulic internal jump? This is possible because the hydraulic jump equation solved by Higuera [15] is nearly the same as it involves a change of pressure associated with the change of the thickness of the film (analogous to δ_1), the inverse of the Froude number being the analog of the buoyancy parameter; furthermore, Higuera [16] solves the problem of a buoyant wall jet over a finite plate with a singularity imposed at the end. His work enters in greater details (influence of adiabatic wall and of Pr number); there is a separation and a back flow as well. The case of cold jet on adiabatic plate leads to separation too; he compares qualitatively this result with what happens in cavity-driven flow where a sort of "hydraulic jump" is observed. Is it nearly impossible to reach the location where $J \simeq -1$ (incidentally, linear stability of the $J \simeq 1$ should be investigated) because branching solutions have appeared far upstream of this point where $J \ll 1$? What are the real downstream boundary conditions? Is it possible to find a set of those boundary conditions which leads to a solution with a region of back flow developing continuously downstream (as proposed by Steinrück in self-similar flows)?

References

[1] N. Afzal, T. Hussain, Mixed convection over a horizontal plate, J. Heat transfer 106 (1984) 240–241.

[2] R.I. Bowles, 1994, Private communication.

[3] R.I. Bowles, F.T. Smith, The standing hydraulic jump: theory, computations and comparisons with experiments, J. Fluid Mech. 242 (1992) 145–168.

[4] P. Bradshaw, T. Cebecci, J.H. Whitelaw, in: Engineering Calculation Methods for Turbulent Flow, Academic Press, New York, 1981.

[5] S.N. Brow, H.K. Cheng Lee, Inviscid viscous interaction on triple deck scales in a hypersonic flow with strong wall cooling, J. Fluid Mech. 220 (1990) 307–309.

[6] S.N. Brown, K. Stewartson, P.G. Williams, A non uniqueness of the hypersonic boundary layer, Q. J. appl. Math. 28, Pt1 (1975) 75–90.

[7] S.N. Brown, K. Stewartson, P.G. Williams, Hypersonic self induced separation, Phys. Fluids 18 (6) (1975).

[8] K.W. Cassel, F.T. Smith, J.D.A. Walker, The onset of instability in unsteady boundary-layer separation, J. Fluid Mech. 315 (1996) 223–256.

[9] S.J. Cowley, L.M. Hocking, O.R. Tutty, The stability of the classical unsteady boundary layer equation, Phys. Fluids 28 (2) (1985).

[10] P.G. Daniels, A singularity in thermal boundary-layer flow on a horizontal surface, J. Fluid Mech. 242 (1992) 419–440.

[11] P.G. Daniels, R.J. Gargaro, Buoyancy effects in stably stratified horizontal boundary-layer flow, J. Fluid Mech. 250 (1993) 233–251.

[12] M. El Hafi, Analyse asymptotique et raccordements, étude d'une couche limite de convection naturelle, thèse de l'Université de Toulouse, 1994.

[13] J. Gajjar, F.T. Smith, On hypersonic self induced separation, hydraulic jumps and boundary layer with algebraic growth, Mathematika 30 (1983) 77–93.

[14] M.G. Hall, The boundary layer over an impulsively started flat plate, Proc. Roy. Soc. A (1969) 401–414.

[15] F.J. Higuera, The hydraulic jump in a viscous laminar flow, J. Fluid Mech. 274 (1994) 62–92.

[16] F.J. Higuera, Opposing mixed convection flow in a wall jet over a horizontal plate, J. Fluid Mech. 342 (1997) 355–375.

[17] P.-Y. Lagrée, Influence of the entropy layer on viscous triple deck hypersonic scales, in: Proceedings of the IUTAM symposium, Aerothermochemestry of spacecraft and associated hypersonic flows, Marseille, France, 1–4 September 1992, pp. 358–361.

[18] P.-Y. Lagrée, Convection thermique mixte à faible nombre de Richardson dans le cadre de la triple couche, C.R. Acad. Sci. Paris t. 318, Série II (1994) 1167–1173.
[19] P.-Y. Lagrée, Upstream influence in mixed convection at small Richardson Number on triple, double and single deck scales, in: Bois, Dériat, Gatignol, Rigolot (Eds.), Symposium on Asymptotic Modelling in Fluid Mechanics, Lecture Notes in Physics, Springer, 1995, pp. 229–238.
[20] P.-Y. Lagrée, Résolution des équations de couche limite interactive instationnaire et applications, Report D.S.P.T.8, février 97, 1997.
[21] J.-C. Le Balleur, Viscid–inviscid coupling calculations for two and three-dimensional flows, Von Kármán Institute for Fluid Dynamics, Comput. Fluid Dynamics Lecture Ser. 1982-04, 1982.
[22] F. Méndez, C. Treviño, A. Liñán, Boundary layer separation by a step in surface temperature, J. Heat Mass Transfer 35 (1992) 2725–2738.
[23] V. Ya Neiland, Propagation of perturbation upstream with interaction between a hypersonic flow and a boundary layer, Mekh. Zhid. Gaz. 4 (1969) 53–57.
[24] V. Ja Neiland, Some features of the transcritical boundary layer interaction and separation, in: Smith, Brow (Eds.), IUTAM Symposium: Boundary Layer Separation, Springer, 1986, pp. 271–293.
[25] A.I. Ruban, S.N. Timoshin, Propagation of perturbations in the boundary layer on the walls of a flat chanel, Fluid Dynamics (2) (1986) 74–79.
[26] A. Ridha, Aiding flows non-unique similarity solutions of mixed-convection boundary-layer equations, Z. Math. Phys. 47 (1996) 341–352.
[27] S. Saintlos, J. Mauss, Asymptotic modelling for separating boundary layers in a channel, Int. J. Eng. Sci. 34 (2) (1996) 201–211.
[28] H. Schlichting, Boundary Layer Theory, seventh ed., McGraw-Hill, New York, 1987.
[29] W. Schneider, A similarity solution for combined forced and free convection flow over a horizontal plate, Int. J. Heat Mass Transfer 22 (1978) 1401–1406.
[30] W. Schneider, M.G. Wasel, Breakdown of the boundary layer approximation for mixed convection above an horizontal plate, Int. J. Heat Mass Transfer 28 (12) (1985) 2307–2313.
[31] F.T. Smith, Flow through constricted or dilated pipes and channels, parts 1 and 2, Q. J. Mech. Appl. Math. 29 (1976) 343–364.
[32] F.T. Smith, On the non parallel flow stability of the Blasius boundary layer, Proc. Roy. Soc. Lond. A 366 (1979) 91–109.
[33] F.T. Smith, On the high Reynolds number theory of laminar flows, IMA J. Appl. Math. 28 (1982) 207–281.
[34] F.T. Smith, J.W. Elliot, On the abrupt turbulent reattachment downstream of leading-edge laminar separation, Proc. Roy. Soc. Lond. A 401 (1985) 1–27.
[35] H. Steinrück, Mixed convection over a cooled horizontal plate: non-uniqueness and numerical instabilities of the boundary layer equations, J. Fluid Mech. 278 (1994) 251–265.
[36] H. Steinrück, Mixed convection over a horizontal plate: self similar and connecting boundary-layer flows, Fluid Dynamic Res. 15 (1995) 113–127.
[37] K. Stewartson, On the impulsive motion of a flat plate in a viscous fluid. II, Q. J. Mech. Appl. Math. 26 Pt2 (1951) 143–152.
[38] K. Stewartson, The theory of laminar boundary layers in compressible fluids, Oxford Math. Monograph (1964).
[39] K. Stewartson, On the impulsive motion of a flat plate in a viscous fluid, Q. J. Mech Appl. Math. 4 Pt2 (1973) 183–198.
[40] K. Stewartson, P.G. Williams, Self-induced separation, Proc. Roy. Soc. A 312 (1969) 181–206.
[41] R.I. Sykes, Stratification effects in boundary layer flows over hills, Proc. Roy. Soc. Lond. A 361 (1978) 225–243.
[42] L. Van Dommeln, S.F. Shen, The spontaneous generation of the singularity in a separating boundary layer, J. Comp. Phys. 38 (1980) 125–140.
[43] M.J. Werle, D.L. Dwoyera, W.L. Hankey, Initial conditions for the hypersonic-shock/boundary-layer interaction problem, AIAA J. 11 (4) (1973) 525–530.